HHS Public Access

Author manuscript

Gastroenterology. Author manuscript; available in PMC 2022 April 01.

Published in final edited form as:

Gastroenterology. 2021 April ; 160(5): 1662–1678.e18. doi:10.1053/j.gastro.2020.12.062.

MiR-10b-5p Rescues Diabetes and Gastrointestinal Dysmotility

Rajan Singh[1,*], **Se Eun Ha**[1,*], **Lai Wei**[1], **Byungchang Jin**[1], **Hannah Zogg**[1], **Sandra M. Poudrier**[1], **Brian G. Jorgensen**[1], **Chanjae Park**[1], **Charles F Ronkon**[1], **Allison Bartlett**[1], **Sung Cho**[1], **Addison Morales**[1], **Yu Heon Chung**[2], **Moon Young Lee**[1,3], **Jong Kun Park**[2], **Andrés Gottfried-Blackmore**[4], **Linda Nguyen**[4], **Kenton M. Sanders**[1], **Seungil Ro**[1,†]

[1]Department of Physiology and Cell Biology, School of Medicine, University of Nevada, Reno, NV, 89557, USA

[2]Division of Biological Sciences, Wonkwang University, Iksan, Chonbuk, Korea

[3]Department of Physiology, Wonkwang Digestive Disease Research Institute and Institute of Wonkwang Medical Science, School of Medicine, Wonkwang University, Iksan, Chonbuk, Korea

[4]Division of Gastroenterology & Hepatology, Stanford University School of Medicine, Stanford, CA, 94305, USA

Abstract

BACKGROUND & AIMS: Interstitial cells of Cajal (ICCs) and pancreatic β cells require receptor tyrosine kinase (KIT) to develop and function properly. Degeneration of ICCs is linked to diabetic gastroparesis. The mechanisms linking diabetes and gastroparesis are unclear, but may involve miRNA mediated post-transcriptional gene silencing in KIT^+ cells.

METHODS: We performed miRNA-seq analysis from isolated ICCs in diabetic mice and plasma from patients with idiopathic and diabetic gastroparesis. miR-10b-5p target genes were identified and validated in mouse and human cell lines. For loss-of-function studies, we used KIT^+ cell-restricted *mir-10b* knockout mice and KIT^+ cell depletion mice. For gain-of-function studies, a

[†]Corresponding author: Seungil Ro, PhD, Associate Professor, Department of Physiology and Cell Biology, University of Nevada School of Medicine, Center of Molecular Medicine Building 207E, 1664 North Virginia Street, MS 352, Reno, NV 89557, Tel: 775-784-1462, Fax: 775-784-6903, sro@med.unr.edu.

[*]These authors contributed equally to this work.

Author contributions

Conceptualization: R.S., S.H., S.R.; methodology: R.S., S.H., L.W., S.M.P.; investigation: R.S., S.H., L.W., B.J., H.Z., C.P., S.C., A.D., Y.H.C., M.Y.L.; writing: R.S., S.H., L.W., H.Z., B.G.J., K.M.S., S.R.; resources: A.G., L.N., J.K.P., K.M.S.; and funding acquisition: S.R.

Supplementary Material

Note: To access the supplementary material accompanying this article, visit the online version of Gastroenterology at www.gastrojournal.org, and at http://doi.org/10.1053/j.gastro.2020.12.062.

Conflict of interest statement (for all authors)

A provisional patent application entitled “miR-10b mimics and targets thereof for use in the treatment of diabetes and gastrointestinal motility disorders” has been filed by S.R. and the University of Nevada Reno Office of Technology Transfer (serial no. 62/837,988, filed April 24 2019).

synthetic miR-10b-5p mimic was injected in multiple diabetic mouse models. We compared the efficacy of miR-10b-5p mimic treatment *vs.* antidiabetic and prokinetic medicines.

RESULTS: miR-10b-5p is highly expressed in ICCs from healthy mice, but drastically depleted in ICCs from diabetic mice. A conditional knockout of *mir-10b* in KIT^+-cells or depletion of KIT^+-cells in mice leads to degeneration of β cells and ICCs, resulting in diabetes and gastroparesis. miR-10b-5p targets the transcription factor Krüppel-like factor 11 (KLF11), which negatively regulates KIT expression. The miR-10b-5p mimic or Klf11 siRNAs injected into *mir-10b* knockout mice, diet-induced diabetic mice, and TALLYHO polygenic diabetic mice rescues the diabetes and gastroparesis phenotype for an extended period of time. Furthermore, the miR-10b-5p mimic is more effective in improving glucose homoeostasis and GI motility as compared with common antidiabetic and prokinetic medications.

CONCLUSIONS: miR-10b-5p is a key regulator in diabetes and gastrointestinal dysmotility via the KLF11-KIT pathway. Restoration of miR-10b-5p may provide therapeutic benefits for these disorders.

Keywords

MicroRNAs; Diabetic gastroparesis; Gastrointestinal dysmotility; Interstitial cells of Cajal; Pancreatic β cells

Introduction

Over 451 million people had diabetes worldwide in 2017.[1] Type 1 diabetes (T1D) develops due to a lack of insulin production by pancreatic β cells, whereas type 2 diabetes (T2D) which accounts for over 95% cases, attributes to increased insulin resistance in the body's cells.[2] T1D and T2D culminate in the degeneration of β cells, requiring insulin therapy.[3] Pathophysiological mechanisms underlying diabetes remain elusive, making it difficult to produce effective treatments that ameliorate the symptoms of diabetes.[4] Moreover, effective treatments for diabetes have been developed; however, many of them are inadequate for prolonged use due to poor tolerance and negative ramifications.[5]

Approximately half of patients with diabetes have gastrointestinal (GI) motility disorders, such as gastroparesis and constipation.[6] GI motility disorders are conditions in which GI muscular movements become abnormal, leading to delayed gastric emptying and slowed colonic transit.[7] GI motility patterns are initiated by the pacemaker activity of interstitial cells of Cajal (ICCs) and neural inputs from enteric motor neurons which are transduced, in part, by ICCs.[8] Hyperglycemia in patients with diabetes leads to the reconfiguration of the mechanisms controlling GI motility,[7] often leading to the dysfunction of ICCs in the stomach and intestines of diabetic animals and humans.[9] ICCs express the receptor tyrosine kinase (KIT), essential for their development and functioning[10] where a loss of KIT leads to non-functional ICCs in diabetic mice, with similar patterns being found in patients with diabetes.[9] However, the underlying mechanisms behind KIT loss in ICCs of patients with diabetes is largely undetermined which prompted us to explore the molecular mechanisms underpinning diabetic GI motility disorders.

microRNAs (miRNAs) are small non-coding regulatory RNAs that mediate post-transcriptional gene repression by inhibiting translation and are master regulators of cell differentiation, proliferation, and apoptosis.[11] Dysregulated miRNAs lead to cellular dysfunction and diseases such as diabetes and GI dysmotility.[12] For example, miR-10b-5p expression is reduced in diabetic patients and animals.[11, 13] Therefore, it is imperative to track the mechanistic pathway at the cellular level to elucidate how miRNAs modulate diabetes and GI motility disorders.

Dysregulation of miR-10b-5p in pancreatic β cells and ICCs might be a potential pathogenic factor leading to the dysfunction of these cells through specific gene target regulation. Krüppel-like factors (KLF) are a family of transcription factors acting as either transcriptional activators or repressors, regulating cellular metabolism.[14] Most KLF isoforms are associated with the regulation of metabolic pathways and energetic homeostasis.[14] KLF11, specifically, regulates insulin production and sensitivity, lipid metabolism, and obesity.[15] Based on these clinical and molecular observations we hypothesized a novel molecular mechanism regulating glucose homeostasis and GI motility through miR-10b-5p mediated KLF11 repression.

In the present study, we found that miR-10b-5p is highly expressed in ICCs from healthy mice and selectively depleted in ICCs from diabetic mice. Using both loss- and gain-of-function studies in mice, we demonstrate that miR-10b-5p regulates both glucose homeostasis and GI motility through the miR-10b-5p-KLF11-KIT pathway. The loss of miR-10b-5p in KIT^{+}-ICCs and β cells causes GI dysmotility and diabetes in mice, while restoring miR-10b-5p expression rescues these conditions. Notably, we found the murine miR-10b-5p-KLF11-mediated KIT regulation data to be consistent with the findings in patients with diabetic and idiopathic gastroparesis. Additionally, we demonstrated that the miR-10b-5p mimic is more efficacious in improving diabetic symptoms and GI functions in diabetic mice when compared to the widely used antidiabetic and prokinetic medications.

Materials and Methods

Note: The full Materials and Methods section is included in the supplementary material.

Mice

All procedures that include animal subjects were approved by the Institutional Animal Care and Use Committee (IACUC) at University of Nevada, Reno (UNR).

Human Specimens

Plasma samples and clinical data were obtained from Stanford University from patients with idiopathic or diabetic gastroparesis along with healthy controls. All human subjects provided informed consent, and all study procedures were approved by Stanford University and UNR Institutional Review Boards.

miRNA Sequencing

Small RNA libraries were generated using an Illumina TruSeq Small RNA Preparation Kit (Illumina) following manufacturer's instructions. The cDNA libraries were sequenced following vendor's instructions.

In vivo Functional GI Motility Tests

Gastric emptying test (GET), total GI transit time (TGITT) and colonic transit time (CTT) were performed on mice fasted overnight. GET was performed using the fluorescent imaging agent GastroSense750 on IVIS Lumina III system. Fluorescence images were analyzed using Living Image software. Evans blue semiliquid solution was orally gavaged in mice to measure TGITT. TGTT was assessed as the time taken from the gavage until the first observation of the blue fecal pellet. CTT was measured through the bead expulsion test.

Construction of Luciferase Reporter and Klf11 Expression Plasmids

For the generation of the luciferase reporter constructs, the miR-10b-hKLF11, miR-10bmKlf11, miR-10b-mKlf11-mut, and scrambled complementary oligonucleotides were synthesized and cloned into the expression vector. All vectors were confirmed by sequencing at the Nevada Genomics Center.

Drug Comparison Study

miR-10b-5p mimic (*In vivo*-jetPEI/miRNA complexes), Metformin, Sitagliptin, Liraglutide, Insulin, and Prucalopride were used for comparing the efficacy for the treatment of metabolic and GI motility conditions in HFHSD-fed C57 male mice.

Statistics

The experimental data are shown as the mean ± SEM. Two-tailed unpaired Student's *t*-test, Mann-Whitney U test, area under the curve calculations, and one-way or two-way ANOVA were used for all mouse and human experiments using GraphPad Prism.

Results

miR-10b Is Suppressed in KIT^{+}-ICCs in Male Diabetic and Obese Mice

To identify abnormally expressed miRNAs in ICCs in diabetes, $Kit^{copGFP/+};Lep^{ob/ob}$ (*ob/ob*) mice were generated.[16] *ob/ob* males significantly gained more weight and had higher fasting blood glucose levels (>250 mg/dL) by 10–12 weeks than their wild type (WT) $Kit^{copGFP/+};Lep^{+/+}$ (+/+) male counterparts (Figure 1A and B). KIT expression has been shown to be regulated by miRNAs,[17] we obtained a miRNA expression profile from isolated colonic and jejunal copGFP^{+} ICCs (CICCs and JICCs) from diabetic *ob/ob* mice and healthy +/+ mice through miRNA-seq (Supplementary Table 1). miRNA expression patterns within *ob/ob* and +/+ CICCs and JICCs were quite different (Figure 1C). The most dynamically expressed miRNAs from both CICCs and JICCs of *ob/ob,* and +/+ mice were shown in Figure 1D. miR-10a-5p, miR-143–3p, and miR10b-5p were the most highly expressed in +/+ ICCs and were substantially decreased in *ob/ob* ICCs. Among these three miRNAs, miR-10b-5p displayed the most substantial diabetes-dependent reduction in diabetic *ob/ob*

ICCs (Figure 1E). Furthermore, we confirmed the diabetes-dependent reduction of miR-10b expression in gastric ICCs from +/+ and *ob/ob* mice by qPCR (Figure 1F). We reinforced previously reported findings that during hyperglycemia the numbers of copGFP$^+$ ICCs in the small intestine and colon were reduced in *ob/ob* males,[16] by demonstrating reduced KIT expression in *ob/ob* males through Western blot (Figure 1G and H).

KIT$^+$ Cell mir-10b Knockout (KO) in Male Mice Results in ICC loss

To determine the functional role of *mir-10b* in ICCs, we generated tamoxifen-inducible KIT$^+$ cell-specific *Kit$^{CreERT2/+}$;mir-10b$^{lox/lox}$* (*mir-10b* KO) mice (Supplementary Figure 1A). We examined the number of ICCs in the jejunum and colon of *mir-10b* KO mice and found that ICCs (CD117$^+$ CD45$^-$) were decreased in the jejunum and colon of *mir-10b* KO mice (Supplementary Figure 1B). The reduction of *mir-10b* was confirmed through qPCR (Supplementary Figure 1C), which showed that miR-10b-5p expression was significantly decreased not only in the jejunum and colon, but also in the pancreas and blood of *mir-10b* KO mice. In the jejunum and colon of *mir-10b* KO mice, KIT protein expression was also decreased (Supplementary Figure 1D and E). Another gene that is potentially regulated by miR-10b-5p is *Klf11*, the evolutionarily conserved metabolic regulator,[18] as it is predicted to have a miR-10b-5p target site in its 3' UTR. KLF11 expression was increased in *mir-10b* KO tissues (Supplementary Figure 1D and E), suggesting that miR-10b-5p may target KLF11. *mir-10b* is encoded within the intronic region of two overlapping genes, *Hoxd3* and *Hoxd4* (Supplementary Figure 1A). We confirmed that the deletion of *mir-10b* did not disrupt the expression of these two genes in *mir-10b* KO mice (Supplementary Figure 1D and E). Additionally, immunohistochemistry showed that the density of ICCs in the deep muscular plexus of the jejunum and along the submucosal surface of the circular muscle layer in the colon was reduced in *mir-10b* KO tissues (Supplementary Figure 1F). Taken together, these results demonstrate that a deficiency of miR-10b-5p in KIT$^+$-ICCs leads to degeneration of jejunal and colonic ICCs. In addition to KIT$^+$-ICCs in the GI tract, miR-10b-5p may also regulate the development of KIT$^+$-β cells in the pancreas linking miR-10b-5p to the diabetic phenotype.

mir-10b KO Male Mice Develop Diabetes and GI Dysmotility

Further, we investigated whether *mir-10b* loss leads to the development of diabetes and GI dysmotility. We found male *mir-10b* KO mice became moderately obese and developed characteristic manifestations of diabetes such as hyperglycemia (blood glucose >200 mg/dL), after 24-weeks post-tamoxifen injection (PTI) (Figure 2A-C), while female *mir-10b* KO mice did not (Supplementary Figure 2A-D). Male *mir-10b* KO mice developed an impaired glucose tolerance after 7-months PTI, while WT mice cleared the glucose efficiently (Figure 2D and E). *mir-10b* KO mice showed reduced fasting blood insulin levels as compared to WT mice (Figure 2F). Furthermore, *mir-10b* KO mice developed insulin resistance after 7-months PTI as compared to WT mice (Figure 2G and H).

Unlike the male dominant diabetic phenotype, both *mir-10b* KO males and females developed gastroparesis and constipation. The *mir-10b* KO males and females showed prolonged total GI transit time (TGITT) starting 1-month PTI which was progressively delayed over a 7-month period. (Figure 2I; Supplementary Figure 2E). Gastric emptying

was also delayed in *mir-10b* KO males and females at 3, 6, and 7 months PTI compared to WT mice (Figure 2J and K; Supplementary Figure 2F and G). Additionally, colonic transit time (CTT), fecal pellet frequency and fecal pellet output in *mir-10b* KO males and females was significantly delayed and reduced, respectively, compared to WT mice (Figure 2L-N; Supplementary Figure 2H). These data suggest that KIT^+ cell-specific *mir-10b* KO male mice developed diabetes and GI dysmotility, while the *mir-10b* KO females only developed GI dysmotility.

Depletion of KIT^+ Cells in Male Mice Results in the Development of Diabetes and GI Dysmotility

To study the role of KIT^+-cells in the pancreas, we generated tamoxifen-induced KIT^+-cell depleted mice, $Kit^{CreERT2/+};Rosa26^{DTA/+}$ (*Kit-DTA*) and fluorescent protein-labeled, $Kit^{CreERT2/+};Rosa26^{tdTom/+}$ (*Kit-tdTom*) mice. KIT^+-cell depleted male mice gained weight and developed characteristic manifestations of diabetes (Supplementary Figure 3A and B). Glucose tolerance tests (GTT) and insulin tolerance tests (ITT) in *Kit-DTA* mice were impaired at 2- and 5-months PTI (Supplementary Figure 3C and D). miR-10b was reduced in the blood of *Kit-DTA* mice at 7-days and 5-months PTI (Supplementary Figure 3E). Consistent with miR-10b reduction, insulin and C-peptide levels were reduced in *Kit-DTA* mice at 7-days and 5-months PTI (Supplementary Figure 3F). Next, we investigated the distribution of KIT^+-cells in the pancreas of *Kit-tdTom* mice. *Kit-tdTom* mice showed an abundance of $tdTom^+$-cells in the pancreas at 7-days PTI (Supplementary Figure 3G). $tdTom^+$-cells were co-labelled with the primary antibody of insulin in islets at 7-days PTI, but few appeared to be $tdTom^+$ 5-months PTI. This implies that β cells may derive from KIT^+-cells and most of the ones that originate from the KIT^+ pancreatic β cell progenitors[19] were lost and replaced with new mature β cells 5-months PTI. Also, β cells ($Insulin^+$-cells) were substantially depleted in *Kit-DTA* mice as compared to *Kit-tdTom* mice. (Supplementary Figure 3G and H). KLF11 levels were increased in the pancreas, colon, and blood of *Kit-DTA* mice at 7-days and 5-months PTI, while KIT expression was reduced (Supplementary Figure 3I and J).

Further, *Kit-DTA* mice displayed delayed TGITT at 2- and 5-months PTI (Supplementary Figure 3K). Collectively, these data show that there are KIT^+-cells located in pancreatic islets and loss of these cells results in depletion of β cells, leading to diabetes. Reduction of miR-10b5p and KIT with subsequent elevation of KLF11 in *Kit-DTA* mice are consistent with results found in *mir-10b* KO mice. Thus, using *mir-10b* KO and *Kit-DTA* mouse models we demonstrated miR-10b-5p likely regulates KIT^+-ICCs in the GI tract and KIT^+-β cells in the pancreas and miR-10b-5p deficiency results in the development of diabetes and GI dysmotility.

MiR-10b-5p Mimic Injection Rescues Diabetes and GI Dysmotility in mir10b KO Male Mice

The synthesized miR-10b-5p duplex (miR-10b-5p mimic) was tested *in vivo* in *mir-10b* KO mice with diabetes and GI dysmotility. Diabetic *mir-10b* KO mice gradually lost weight over the first 4-weeks post-injection (PI) with the miR-10b-5p mimic, while the scramble RNA negative control and non-injected mice did not lose weight (Figure 3A). The reduced body weight was maintained in miR-10b-5p mimic-injected mice for 10-weeks PI. More

importantly, miR-10b-5p mimic-injected mice dramatically lowered fasting glucose levels to normal (about 100 mg/dL) at 1-week PI and maintained the healthy levels for 8-weeks (Figure 3B). We compared fasting and glucose stimulated insulin levels between *mir-10b* KO mice injected with the miR-10b-5p mimic 1-week PI, no injection, and scramble injection (Figure 3C). Fasting insulin levels were restored in *miR10b* KO mice 1-week PI with the miR-10b-5p mimic as compared to *mir-10b* KO mice with no injection or scramble injection. Furthermore, the pattern of glucose stimulated insulin levels in the *mir-10b* KO mice injected with the miR-10b-5p mimic was similar to that in WT mice (Figure 3C). Glucose and insulin tolerance were significantly improved in the miR-10b-5p mimic-injected mice (Figure 3D-G). Furthermore, GI motility was gradually improved to normal levels in the miR-10b-5p mimic-injected mice at 2- and/or 4-weeks PI (Figure 3H-J). We confirmed that miR-10b-5p was increased in the blood, pancreas, jejunum and colon 1-week PI of the miR10b-5p mimic (Figure 3K). KIT and KLF11 protein expression were dysregulated in the pancreas and colon of *mir-10b* KO mice, but their protein levels were partially restored after 1week in the miR-10b-5p mimic-injected mice (Figure 3L and M). ICCs were degenerated in the *mir-10b* KO diabetic mice but readily detected after 1-week in the jejunum and colon of mice injected with the miR-10b-5p mimic (Figure 3N). These data demonstrate that the miR-10b-5p mimic injection reversed diabetic symptoms and GI dysmotility in *mir-10b* KO male mice.

MiR-10b-5p Mimic Rescues Diabetes and GI Dysmotility in Multiple Diabetic Mouse Models

We next evaluated metabolic and/or GI motility parameters to test the effect of the miR-10b5p mimic on several diabetic mouse models [(High-fat, high-sucrose diet (HFHSD)-induced C57 male, HFHSD-fed ovariectomized (OVX) C57 female, *ob/ob* and TALLYHO male mice]. HFHSD-fed mice became obese and hyperglycemic compared to normal diet (ND)-fed mice (Figure 4A and B). The HFHSD-fed mice significantly lost weight and displayed a marked reduction in fasting blood glucose levels PI of the miR-10b-5p mimic compared to ND-fed mice (Figure 4A and B). The first miR-10b-5p mimic injection lowered blood glucose to normal levels, which returned to pre-diabetic levels 5-weeks PI. A second miR-10b-5p mimic injection lowered glucose to normal levels for an additional 6-weeks. In addition, TGITT and fecal output were restored in HFHSD-fed mice injected with miR-10b-5p mimic 4-weeks post-second injection (Figure 4C and D). miR-10b-5p expression was substantially reduced in the blood of diabetic HFHSD-fed mice (Figure 4E). miR-10b-5p levels were restored to approximately 60% of the healthy level following miR-10b-5p mimic injection at 1-week PI and gradually decreased (Figure 4E). Insulin levels were restored 1-week PI with miR-10b-5p mimic, following a similar pattern to the level of miR-10b-5p in the blood from HFHSD-fed mice (Figure 4F). Hemoglobin A1C (A1C) levels in HFHSD-fed mice were also improved by miR-10b-5p mimic (Figure 4G). KLF11 levels were increased in the blood, pancreas, stomach, colon, and skeletal muscle of HFHSD-fed mice (Figure 4H and I). miR-10b-5p mimic treatment reduced KLF11 expression and, in turn, increased KIT expression in the tissues of HFHSD-fed mice 3-weeks PI (Figure 4H and I). KIT^+-ICCs were degenerated in HFHSD-fed mice, but KIT expression was restored in the stomach, jejunum, and colon 1-week PI with miR-10b-5p mimic (Figure 4J). Pancreatic islets were also reduced in size in HFHSD-fed mice; however, some islets were restored 1-week PI with miR-10b-5p mimic in HFHSD-fed

mice (Figure 4K). These data demonstrate that miR-10b5p mimic injection likely restores proper functioning of ICCs and β cells by increasing the expression of KIT and insulin in HFHSD-fed male mice, which leads to the reversal of GI dysmotility and diabetes.

Estrogen delays the onset of diabetes in female mice.[20] Therefore, we evaluated the effect of the miR-10b-5p mimic on HFHSD-fed OVX female diabetic mice, as the *mir-10b KO* mice in this study as well as mice from other murine studies demonstrated HFD-fed female mice do not develop hyperglycemia.[20] OVX C57 female HFHSD-fed mice substantially lost estrogen, gained weight, and became hyperglycemic (Supplementary Figure 4). Injection with the miR-10b-5p mimic in OVX HFHSD-fed females reversed the diabetic phenotype, while maintaining the body weight (Supplementary Figure 4E-F).

Further, we tested the efficacy of the miR-10b mimic in rescuing the diabetic and GI dysmotility phenotypes in diabetic *ob/ob* and polygenic TALLYHO T2D male mice. Both *ob/ob*- and TALLYHO male mice injected with the miR-10b mimic were able to significantly lower blood glucose and improve TGITT (Supplementary Figure 5 and 6).

MiR-10b-5p Regulates Expression of KIT via KLF11

To identify the underlying molecular mechanisms in miR-10b-5p-KLF11-KIT pathway, we searched for miR-10b-5p target genes associated with diabetes utilizing Ingenuity Pathway Analysis (IPA). IPA identified 44 miR-10b-5p targets directly linked to diabetes (Figure 5A). As KLF11 directly interacts with the insulin (INS) gene by inhibiting its promoter activity in β cells,[21] we next examined the targeting effect of miR-10b-5p on KLF11 in the human (Panc.10.05) and mouse (NIT-1) pancreatic β cell lines. We tested the miR-10b-5p mimic and its antisense RNA (miR-10b-5p inhibitor) in these two β cell lines (Figure 5B). Western blots depicted that miR10b-5p mimic transfection decreased KLF11 levels, while the miR-10b-5p inhibitor increased KLF11 levels in these cell lines (Figure 5C and D). KIT and INS expression was inversely regulated by the miR-10b-5p mimic and inhibitor. Expression of these two proteins was also augmented by transfection with the KLF11 siRNAs (siKLF11–1 and siKLF11–2), substantiating miR-10b-5p regulates expression of KIT and INS via KLF11(Figure 5C and D). The miR-10b-5p targeting effect on KLF11 was further validated in β cell lines, transfected with plasmids containing the luciferase gene with the 3’ UTR of KLF11 (human and mouse) miR-10b target site (TS), a target site mutation (TSM) or a scramble sequence (Figure 5E). Each cell line was transfected with mKlf11 miR-10b TS and TSM or hKLF11 miR-10b TS plasmids and then subsequently treated with different concentrations of miR-10b mimic or inhibitor. All treatments showed a respective dose-dependent reduction or induction of luciferase activity (Figure 5F). The expression of miR-10b-5p was reduced by the high glucose level (Figure 5G), which also affected KLF11 and KIT protein expression in NIT-1 cells (Figure 5H and I). A similar targeting effect on luciferase activity by high glucose levels was observed in both mouse and human β cell lines (Figure 5J). These data imply miR-10b-5p targets and inhibits the expression of KLF11, which subsequently suppresses the expression of KIT and INS in β cells. Next, we examined whether the Klf11 siRNAs could rescue diabetes and slowed GI transit in HFHSD-fed male mice. Diabetic, obese, and GI dysmotility phenotypes were substantially rescued by Klf11 siRNA. (Supplementary Figure 7). Taken together,

miR-10b-5p mimic can reverse diabetic, obese, and GI dysmotility phenotypes via the suppression of Klf11.

Patients with Diabetic and Idiopathic Gastroparesis Have Reduced miR10b-5p Expression

We examined plasma samples from patients with diabetic gastroparesis (DG) and idiopathic gastroparesis (IG) (Supplementary Table 2) to see whether the abnormal expression patterns of miR-10b-5p, KLF11, and KIT were similar to what we observed in our animal models. miR-10b5p expression was high in the healthy control (HC) samples and reduced in IG and DG samples (Figure 6A). Based on the miR-10b-5p expression levels, we found two groups of IG: intermediate-high expression (IG-H) and intermediate-low expression (IG-L). miR-10b-5p expression was low in DG samples. Consistent with our murine data, insulin, C-peptide, A1C levels and expression profiles of miR-10b-5p, KLF-11, and KIT were similar in the patient samples (Figure 6B-E). The IG-L group had significantly lower levels of miR-10b-5p, insulin and C-peptide compared to those of the HC group but had higher expression levels than the DG group, suggesting the IG-L group is at a prediabetic stage. Deep sequencing of miRNAs from the blood samples of HC, IG-H, IG-L, and DG identified differentially expressed miRNAs (Supplementary Table 3). The expression patterns of all of the 345 identified miRNAs and the top 70 most dynamically regulated miRNAs show similarity between HC and IG-H and between IG-L and DG (Figure 6F and G). miR-10b-5p levels were highest in HC, followed by IG-H, IG-L, & DG, respectively (Figure 6G). In addition, expression levels of miR-10b-5p were negatively correlated with gastric emptying scintigraphy percentage at 2-hrs in gastroparesis as well as with A1C levels in diabetes (Figure 6H). Taken together, metabolic and gene expression profiles from HC, IG, and DG patient samples were analogous to our mouse data.

Efficacy Comparison of the miR-10b-5p Mimic with Antidiabetic and Prokinetic Drugs

We next compared the effects of miR-10b-5p mimic on diabetes and GI dysmotility in HFHSD-fed C57 mice with antidiabetic medications (liraglutide, sitagliptin, metformin, and insulin) and a prokinetic medication, prucalopride (Figure 7A). miR-10b-5p mimic injections (2 doses of IP) into HFHSD-induced diabetic mice reduced body weight and rescued the hyperglycemic condition. Antidiabetic medications and prucalopride lowered blood glucose, but the efficacy and duration were lower and shorter than that of miR-10b-5p mimic (Figure 7B and C). Glucose and insulin tolerance were improved in miR-10b-5p mimic-injected mice for up to 8- weeks with two injections, while the medications only maintained improvement for 4-weeks after treatment (Figure 7D and E). Fasting insulin and C-peptide levels in mice treated with the medications and miR-10b-5p mimic were increased at 4-weeks (Supplementary Figure 8A and B). Glucose stimulated insulin secretion was significantly impaired in HFHSD-mice but was restored and maintained in mice injected with the miR-10b-5p mimic for 8-weeks (Figure 7F). In addition, GI motility was restored in miR-10b-5p mimic-injected mice for 8-weeks PI, while prucalopride improved GI motility for only 4-weeks. (Figure 7G-I; Supplementary Figure 8C). Next, we examined other metabolic parameters (food, calorie, and water intake, urine and fecal output) and found that the mir-10b-5p mimic-injected mice have better control of symptoms such as polyphagia, polydipsia, and polyuria (Supplementary Figure 9). Taken together, these murine metabolic

and GI motility data confirm the profound and prolonged efficacy of miR-10b mimic as compared to antidiabetic and prokinetic medications.

Discussion

Diabetes and gastroparesis are phenotypically associated, however, a defined network of molecular mechanisms has yet to be unveiled. This study revealed that deficiency of miR-10b5p in KIT$^+$-cells (ICCs and pancreatic β cell progenitors) contributes to the development of GI motility disorders and diabetes via transcription factor, KLF11. Removal of *mir-10b* in KIT$^+$-cells caused cellular degeneration, which triggered the onset of GI dysmotility and diabetes. Treatment of diabetic mice with a miR-10b-5p mimic reversed the diabetic and GI dysmotility phenotypes.

Our data suggest that diabetes and gastroparesis can develop due to the degeneration of ICCs and β cells, both caused by the lack of miR-10b-5p. Previous studies have shown that ICCs require stem cell factor and KIT signaling for proper growth and function.[22] It is widely accepted that loss of KIT in ICCs results in abnormal GI motility in animals, and ICC loss is also associated with GI motility disorders in humans.[23] However, the pathogenic factor leading to KIT loss in ICCs was elusive until now. Our *mir-10b* KO mice demonstrated that decreased miR10b-5p levels lead to reduced KIT expression and subsequent degeneration of ICCs resulting in delayed gastric emptying as well as slowed colonic and total GI transit. Meanwhile, murine studies demonstrated the importance of KIT in glucose homeostasis.[24] Loss of KIT activity in pancreatic β cells in Kit^{Wv} mutant mice resulted in decreased β cell proliferation and hyperglycemia,[25] while KIT overexpression in $Kit^{\beta Tg}$ mice prevented HFD-induced diabetes.[24] KIT$^+$-cells serve as pancreatic β cell progenitors and cells derived from KIT$^+$-cells are insulin-producing β cells.[26] *Kit-DTA* mice developed a diabetic phenotype due to ablation of KIT$^+$ pancreatic β cells. Our findings confirmed that the loss of miR-10b in KIT$^+$-cells (β cells and ICCs) in *mir-10b* KO mice lead to the co-occurrence of diabetes and GI dysmotility. Further investigation is warranted to elucidate if other pathogenic changes (dysregulation of immune cells, enteric neurons, and adipocytes) have a co-occurrence with degenerated KIT$^+$ cells in the *mir-10b* KO diabetic and GI dysmotility model.

The diabetic phenotype in our mouse models (*mir-10b* KO and HFHSD-induced mice) was apparent in males, but not females. Likewise, this gender bias is also true in humans.[27] Diabetes is more common in males ≤45 yrs old, while it is the reverse in females ≥45 yrs old due to the depletion of estrogen.[28] Estrogen protects rodent pancreatic β cells *in vivo* against multiple pro-apoptotic insults and this protection is conserved in human islets.[20, 29] This gender/age nexus to diabetes suggests that estrogen hormone therapy may reduce the incidence of T2D by protecting β cell function in post-menopausal women.[30] We confirmed HFHSD-fed OVX female mice developed diabetes similar to males. Furthermore, we demonstrated that the diabetes phenotype was rescued by the miR-10b mimic in both male and female mice. Future studies are warranted to enumerate the linkage between sexual dimorphism/estrogen levels and diabetes. Unlike the diabetic phenotype, both male and female *mir-10b* KO mice developed gastroparesis. Additionally, these mice developed slow transit constipation, which is consistent with recent data from patients with gastroparesis

showing an overlap of approximately 60–70% with slow transit constipation.[31] This suggest our conditional *mir-10b* KO mouse is a good model to study diabetic and idiopathic gastroparesis.

Our data suggested that *mir-10b* is required for the survival, proper growth and function of KIT^+-ICCs and KIT^+-β cells. We confirmed the restoration of KIT in ICCs and β cells after miR10b-5p mimic injections in mice with diabetes and GI dysmotility. miR-10b-5p mimic injections were also able to lower blood glucose levels for up to 10-weeks after a single injection, with significant improvements in GI motility. Further, miR-10b-5p mimic injections were able to reduce and maintain body weight reduction for up to 10-weeks in HFHSD-induced diabetic and obese mice. However, it is not clear how miR-10b-5p regulates β-cell function and tissue specific insulin sensitivity, which are required for further studies using cell-specific animal models.

This study showed miR-10b regulates three phenotypes: hyperglycemia, GI dysmotility, and obesity. However, unlike how diabetes and GI dysmotility were directly regulated by miR-10b-5p via KIT^+-β-cell and ICCs, the obesity phenotype is likely only a secondary effect because it developed after the hyperglycemia and GI dysmotility phenotypes. This suggests the weight gain was likely due to complications caused by the diabetic phenotype (changed glucose and insulin levels). Further studies are warranted to investigate the molecular mechanisms linking these three pathological phenotypes using cell- or tissue-specific KO animal models.

miRNAs are excellent diagnostic markers for diseases.[32] Our data showed that miR-10b-5p is highly expressed in ICCs from healthy mice but markedly reduced in ICCs from diabetic mice. Furthermore, we demonstrated reduced expression of miR-10b-5p in blood from mice with diabetes and GI dysmotility. The later was in conjunction with reduced expression of miR-10b5p in patients with DG and IG. The reduced miR-10b-5p expression profile for mice and humans was consistent with the miRNA expression profiles of diabetic rats,[33] HFD-induced hepatic insulin-resistant mice,[11] children with T1D[34] and twins with T2D.[13] Thus, we suggest the use of miR-10b-5p as a potential diagnostic marker for diabetes/GI motility disorders.

Overexpression of miR-10b-5p is linked to many cancer types and has also been shown to promote cell proliferation and migration.[35] In parallel, miR-10b-5p is highly expressed in proliferating stem cell lines,[36] suggesting they likely have a role in the proliferation of KIT^+-ICCs and β cells. Injection of miR-10b-5p in mice may induce cancer development; however, we confirmed there was no indication of cancer development in miR-10b-5p mimic (500 ng/g) injected mice over a one-year period. This suggests that a low dose of the miRNA mimic is not enough to induce cancer. Further, we showed a single injection of the miR-10b-5p mimic into mice restored miR-10b-5p in blood to approximately 40–60% of healthy levels, but not to the elevated levels reported in cancers.[35] Therefore, it is unlikely that the miR-10b-5p mimic injections will lead to cancer development when used to treat diabetes and GI dysmotility caused by reduced miR-10b-5p expression.

Our study demonstrated a novel mechanistic pathway miR-10b-5p-KLF11-KIT in the regulation of glucose homeostasis and GI motility. We confirmed that miR-10b-5p mimic has targeting effects on KLF11 (using both mouse and human β cell lines) and demonstrated that expression of KIT is negatively regulated by KLF11, the metabolic regulator controlling multiple pathways attributed to diabetes and its early onset.[14] A congenital deletion of *Klf11* in mice results in decreased blood glucose levels and body weight, as well as protection against HFD-induced obesity and diabetes,[15] similar to what we found after injection of the miR-10b-5p mimic and Klf11 siRNAs. Binding of KLF11 to GC and CACCC boxes at the promoter of proinsulin gene *INS* suppresses transcriptional activation.[37] KLF11 recruits transcriptional repressor SIN3A and epigenetic gene silencers HDAC1/2 and HP1, which may silence INS and KIT genes in diabetes and GI dysmotility.[38]

Unlike antidiabetic drugs, such as GLP-1 agonists and metformin, that causes delayed GI motility as a side effect,[39] miR-10b-5p mimic treatment reversed the GI dysmotility phenotype. Prolonged exposure to current antidiabetic medications such as metformin can lead to progressive β cell failure and increased insulin resistance,[5] while the miR-10b-5p mimic treatment restored glucose tolerance and insulin sensitivity. Our drug comparison study with the miR-10b-5p mimic depicted a compelling long-term efficacy in reversing the phenotypes of both diabetes and GI dysmotility when compared to commonly used antidiabetic and prokinetic medications. The beneficial and prolonged effects as seen with the use of the miR-10b-5p mimic in both diabetes and GI dysmotility suggest an opportunity for a new therapeutic approach. By restoring miR-10b-5p in these disease states, we may be able to attenuate symptoms and restore key cells detrimental for insulin production and GI motility, while additionally alleviating the burden for patents relying on insulin treatments.

Supplementary Material

Refer to Web version on PubMed Central for supplementary material.

Acknowledgments

We would like to thank Fadi Hendee, M.D. for providing his clinical knowledge, Benjamin J Weigler, D.V.M. and Walt Mandeville, D.V.M. for their excellent animal services provided to the mice, as well as Ellen Purpus and Mridul Gautam for their outstanding research support.

Grant support

Research was supported by YUYANG DNU No. 1800616, NIDDK (DK091725, DK094886,

DK103055 to S. Ro, and P01 DK41315 to K. Sanders and S. Ro)

Abbreviations used in this paper:

CTT
colonic transit time

DG
diabetic gastroparesis

GCSI-dd

gastroparesis cardinal symptom index-daily diary

GET
gastric emptying test

GTT
glucose tolerance test

HFHSD
high fat high sucrose diet

ICC
interstitial cell of Cajal

IG
idiopathic gastroparesis

IP
intraperitoneal

ITT
insulin tolerance test

KLF11
Krüppel-like factors

KIT
receptor tyrosine kinase

Kit-DTA
Kit$^{CreERT2/+}$

Rosa26$^{DTA/+}$

Kit-tdTom
Kit$^{CreERT2/+}$

Rosa26$^{tdTom/+}$

ob/ob
Kit$^{copGFP/+}$

Lep$^{ob/ob}$

OVX
ovariectomized

PI
post-injection

PO
per oral

PTI
post-tamoxifen injection

SC
subcutaneous

TGITT
total gastrointestinal transit time

References

1. Cho NH, Shaw JE, Karuranga S, et al. IDF Diabetes Atlas: Global estimates of diabetes prevalence for 2017 and projections for 2045. Diabetes Res Clin Pract 2018;138:271–281. [PubMed: 29496507]
2. Holman N, Young B, Gadsby R. Current prevalence of Type 1 and Type 2 diabetes in adults and children in the UK. Diabet Med 2015;32:1119–20. [PubMed: 25962518]
3. Halban PA, Polonsky KS, Bowden DW, et al. beta-cell failure in type 2 diabetes: postulated mechanisms and prospects for prevention and treatment. Diabetes Care 2014;37:1751–8. [PubMed: 24812433]
4. Eizirik DL, Pasquali L, Cnop M. Pancreatic beta-cells in type 1 and type 2 diabetes mellitus: different pathways to failure. Nat Rev Endocrinol 2020;16:349–362.
5. Cherney DZI, Lam TKT. A Gut Feeling for Metformin. Cell Metab 2018;28:808–810. [PubMed: 30517894]
6. Camilleri M, Chedid V, Ford AC, et al. Gastroparesis. Nat Rev Dis Primers 2018;4:41. [PubMed: 30385743]
7. Bharucha AE, Kudva YC, Prichard DO. Diabetic Gastroparesis. Endocr Rev 2019.
8. Sanders KM, Ward SM, Koh SD. Interstitial cells: regulators of smooth muscle function. Physiol Rev 2014;94:859–907. [PubMed: 24987007]
9. Grover M, Bernard CE, Pasricha PJ, et al. Clinical-histological associations in gastroparesis: results from the Gastroparesis Clinical Research Consortium. Neurogastroenterol Motil 2012;24:531–9, e249. [PubMed: 22339929]
10. Beckett EA, Ro S, Bayguinov Y, et al. . Kit signaling is essential for development and maintenance of interstitial cells of Cajal and electrical rhythmicity in the embryonic gastrointestinal tract. Dev Dyn 2007;236:60–72. [PubMed: 16937373]
11. Croce CM, Calin GA. miRNAs, cancer, and stem cell division. Cell 2005;122:6–7. [PubMed: 16009126]
12. Mazzone A, Strege PR, Gibbons SJ, et al. microRNA overexpression in slow transit constipation leads to reduced NaV1.5 current and altered smooth muscle contractility. Gut 2020;69:868–876. [PubMed: 31757880]
13. Bork-Jensen J, Scheele C, Christophersen DV, et al. Glucose tolerance is associated with differential expression of microRNAs in skeletal muscle: results from studies of twins with and without type 2 diabetes. Diabetologia 2015;58:363–73. [PubMed: 25403480]
14. Pollak NM, Hoffman M, Goldberg IJ, et al. Kruppel-like factors: Crippling and un-crippling metabolic pathways. JACC Basic Transl Sci 2018;3:132–156. [PubMed: 29876529]

15. Mathison A, Escande C, Calvo E, et al. Phenotypic Characterization of Mice Carrying Homozygous Deletion of KLF11, a Gene in Which Mutations Cause Human Neonatal and MODY VII Diabetes. Endocrinology 2015;156:3581–95. [PubMed: 26248217]
16. Ro S, Park C, Jin J, et al. A model to study the phenotypic changes of interstitial cells of Cajal in gastrointestinal diseases. Gastroenterology 2010;138:1068–78 e1–2. [PubMed: 19917283]
17. Fan R, Zhong J, Zheng S, et al. MicroRNA-218 inhibits gastrointestinal stromal tumor cell and invasion by targeting KIT. Tumour Biol 2014;35:4209–17. [PubMed: 24375253]
18. Lomberk G, Grzenda A, Mathison A, et al. Kruppel-like factor 11 regulates the expression of metabolic genes via an evolutionarily conserved protein interaction domain functionally disrupted in maturity onset diabetes of the young. J Biol Chem 2013;288:17745–58. [PubMed: 23589285]
19. Feng ZC, Riopel M, Popell A, et al. A survival Kit for pancreatic beta cells: stem cell factor and c-Kit receptor tyrosine kinase. Diabetologia 2015;58:654–65. [PubMed: 25643653]
20. Xu B, Allard C, Alvarez-Mercado AI, et al. Estrogens Promote Misfolded Proinsulin Degradation to Protect Insulin Production and Delay Diabetes. Cell Rep 2018;24:181–196. [PubMed: 29972779]
21. Niu X, Perakakis N, Laubner K, et al. Human Kruppel-like factor 11 inhibits human proinsulin promoter activity in pancreatic beta cells. Diabetologia 2007;50:1433–41. [PubMed: 17479246]
22. Maeda H, Yamagata A, Nishikawa S, et al. Requirement of c-kit for development of intestinal pacemaker system. Development 1992;116:369–75. [PubMed: 1283735]
23. Sanders KM, Koh SD, Ro S, et al. Regulation of gastrointestinal motility--insights from smooth muscle biology. Nat Rev Gastroenterol Hepatol 2012;9:633–45. [PubMed: 22965426]
24. Feng ZC, Li J, Turco BA, et al. Critical role of c-Kit in beta cell function: increased insulin secretion and protection against diabetes in a mouse model. Diabetologia 2012;55:2214–25. [PubMed: 22581040]
25. Krishnamurthy M, Ayazi F, Li J, et al. . c-Kit in early onset of diabetes: a morphological and functional analysis of pancreatic beta-cells in c-KitW-v mutant mice. Endocrinology 2007;148:5520–30. [PubMed: 17673521]
26. Ma F, Chen F, Chi Y, et al. Isolation of pancreatic progenitor cells with the surface marker of hematopoietic stem cells. Int J Endocrinol 2012;2012:948683.
27. Menke A, Casagrande S, Geiss L, et al. Prevalence of and Trends in Diabetes Among Adults in the United States, 1988–2012. JAMA 2015;314:1021–9. [PubMed: 26348752]
28. Wang WS, Wahlqvist ML, Hsu CC, et al. Age- and gender-specific population attributable risks of metabolic disorders on all-cause and cardiovascular mortality in Taiwan. BMC Public Health 2012;12:111. [PubMed: 22321049]
29. Tiano JP, Mauvais-Jarvis F. Importance of oestrogen receptors to preserve functional beta-cell mass in diabetes. Nat Rev Endocrinol 2012;8:342–51. [PubMed: 22330739]
30. Mauvais-Jarvis F, Manson JE, Stevenson JC, et al. Menopausal Hormone Therapy and Type 2 Diabetes Prevention: Evidence, Mechanisms, and Clinical Implications. Endocr Rev 2017;38:173–188. [PubMed: 28323934]
31. Zikos TA, Kamal AN, Neshatian L, et al. High Prevalence of Slow Transit Constipation in Patients With Gastroparesis. J Neurogastroenterol Motil 2019;25:267–275. [PubMed: 30870880]
32. Vasu S, Kumano K, Darden CM, et al. MicroRNA Signatures as Future Biomarkers for Diagnosis of Diabetes States. Cells 2019;8.
33. Herrera BM, Lockstone HE, Taylor JM, et al. Global microRNA expression profiles in insulin target tissues in a spontaneous rat model of type 2 diabetes. Diabetologia 2010;53:1099–109. [PubMed: 20198361]
34. Samandari N, Mirza AH, Kaur S, et al. Influence of Disease Duration on Circulating Levels of miRNAs in Children and Adolescents with New Onset Type 1 Diabetes. Noncoding RNA 2018;4.
35. Sheedy P, Medarova Z. The fundamental role of miR-10b in metastatic cancer. Am J Cancer Res 2018;8:1674–1688. [PubMed: 30323962]
36. Guessous F, Alvarado-Velez M, Marcinkiewicz L, et al. Oncogenic effects of miR-10b in glioblastoma stem cells. J Neurooncol 2013;112:153–63. [PubMed: 23307328]

37. Neve B, Fernandez-Zapico ME, Ashkenazi-Katalan V, et al. Role of transcription factor KLF11 and its diabetes-associated gene variants in pancreatic beta cell function. Proc Natl Acad Sci U S A 2005;102:4807–12. [PubMed: 15774581]

38. Lomberk G, Mathison AJ, Grzenda A, et al. . Sequence-specific recruitment of heterochromatin protein 1 via interaction with Kruppel-like factor 11, a human transcription factor involved in tumor suppression and metabolic diseases. J Biol Chem 2012;287:1302639.

39. Sato D, Morino K, Nakagawa F, et al. Acute Effect of Metformin on Postprandial Hypertriglyceridemia through Delayed Gastric Emptying. Int J Mol Sci 2017;18. Author names in bold designate shared co-first authorship

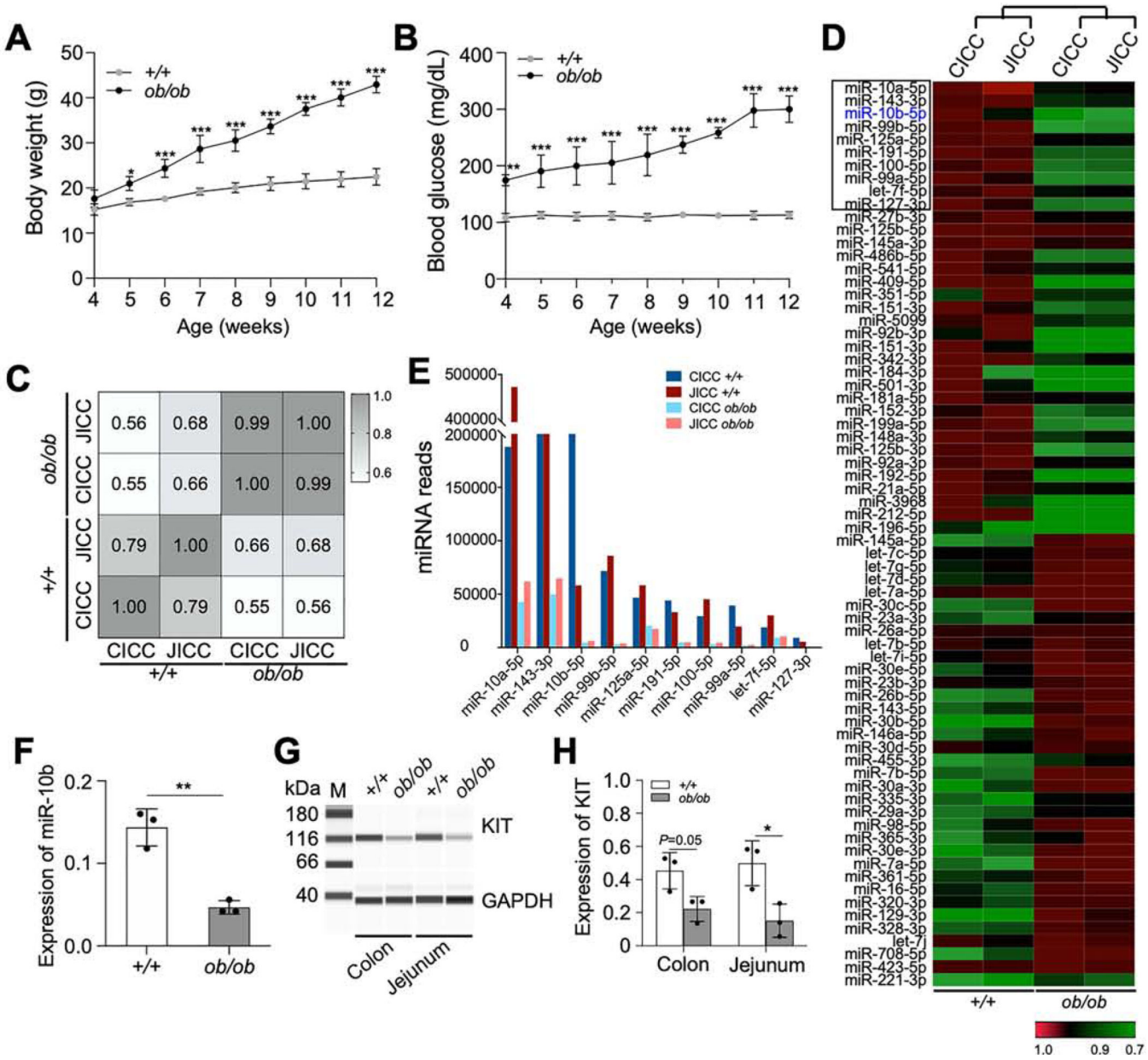

Figure 1.

Expression of miR-10b-5p is drastically reduced in KIT^{+}-ICCs in male diabetic *Kit*$^{copGFP/+}$;*Lep*$^{ob/ob}$ Mice. (*A, B*) Body weight and fasting blood glucose levels of *Kit*$^{copGFP/+}$;*Lep*$^{+/+}$ (+/+) and *Kit*$^{copGFP/+}$;*Lep*$^{ob/ob}$ (*ob/ob*) mice (Two-way ANOVA, n=8). (*C*) Pearson correlation analysis between miRNA-seq data obtained from colonic and jejunal ICC (CICC and JICC, respectively) isolated and pooled from diabetic *ob/ob* (n=30) and +/+ mice (n=20). (*D*) Heat map of the 70 most dynamically regulated miRNAs in CICC and JICC of diabetic *ob/ob* mice. (*E*) Expression levels of the ten most prominently reduced miRNAs in CICC and JICC of diabetic *ob/ob* mice from panel E (black box) obtained by miRNA-seq (n=20–30). (*F*) Expression of miR10b-5p in gastric ICCs of +/+ and *ob/ob* mice measured by qPCR (n=3). (*G, H*) Western blot and quantification of KIT in the jejunum and

colon of +/+ and *ob/ob* mice (n=3). Error bar indicate SEM, unpaired *t*-test. *$p < 0.05$, **$p < 0.01$.

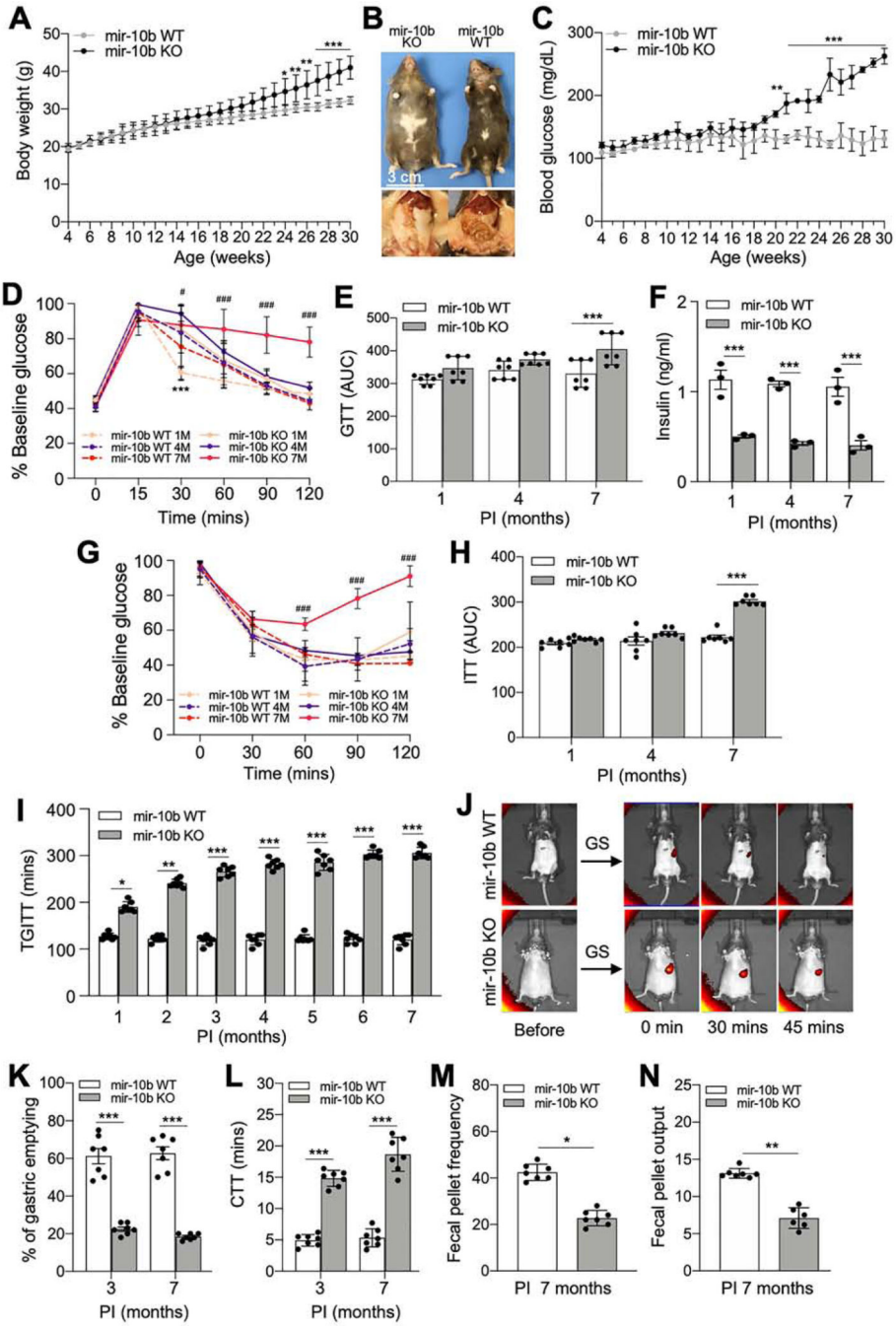

Figure 2.

Male KIT^{+} cell-specific *mir-10b* KO mice develop diabetes and GI dysmotility. *Kit*$^{CreERT2/+}$;*mir-10b*$^{lox/lox}$ mice were injected with tamoxifen (*mir-10b* KO) or oil (*mir-10b* WT) at 4-weeks of age. (*A*) Body weight of *mir-10b* KO and WT male mice. (*B*) Gross anatomical images of 30-weeks old male *mir-10b* KO and WT mice. (*C*) Fasting blood glucose levels in *mir-10b* KO and WT male mice. (*D*) Glucose tolerance tests (GTT) in *mir-10b* KO and WT male mice. (*E*) GTT plot of the area under the curve (AUC) from (*D*). (*F*) Changes in blood insulin levels after 6-hrs fasting in *mir-10b* KO and WT male

mice (n=3). (*G*) Insulin tolerance test (ITT) in *mir-10b* KO and WT male mice. (*H*) ITT plot of the AUC from (*G*). (*I*) Total GI transit time (TGITT). (*J*) Gastric emptying images of 7-month-old *mir-10b* KO and WT mice. (*K*) Quantification of gastric emptying at 30-min. (*L*) Colonic transit time (CTT). (*M, N*) Fecal pellet frequency and output within 24-hrs. (unpaired *t*-test). n=7 per condition for each experiment. Error bar indicate SEM, Two-way ANOVA. $*p < 0.05$, $**p < 0.01$, $***p < 0.001$, $^{\dagger\dagger}p < 0.01$, $^{\#}p < 0.05$, $^{\#\#\#}p < 0.001$.

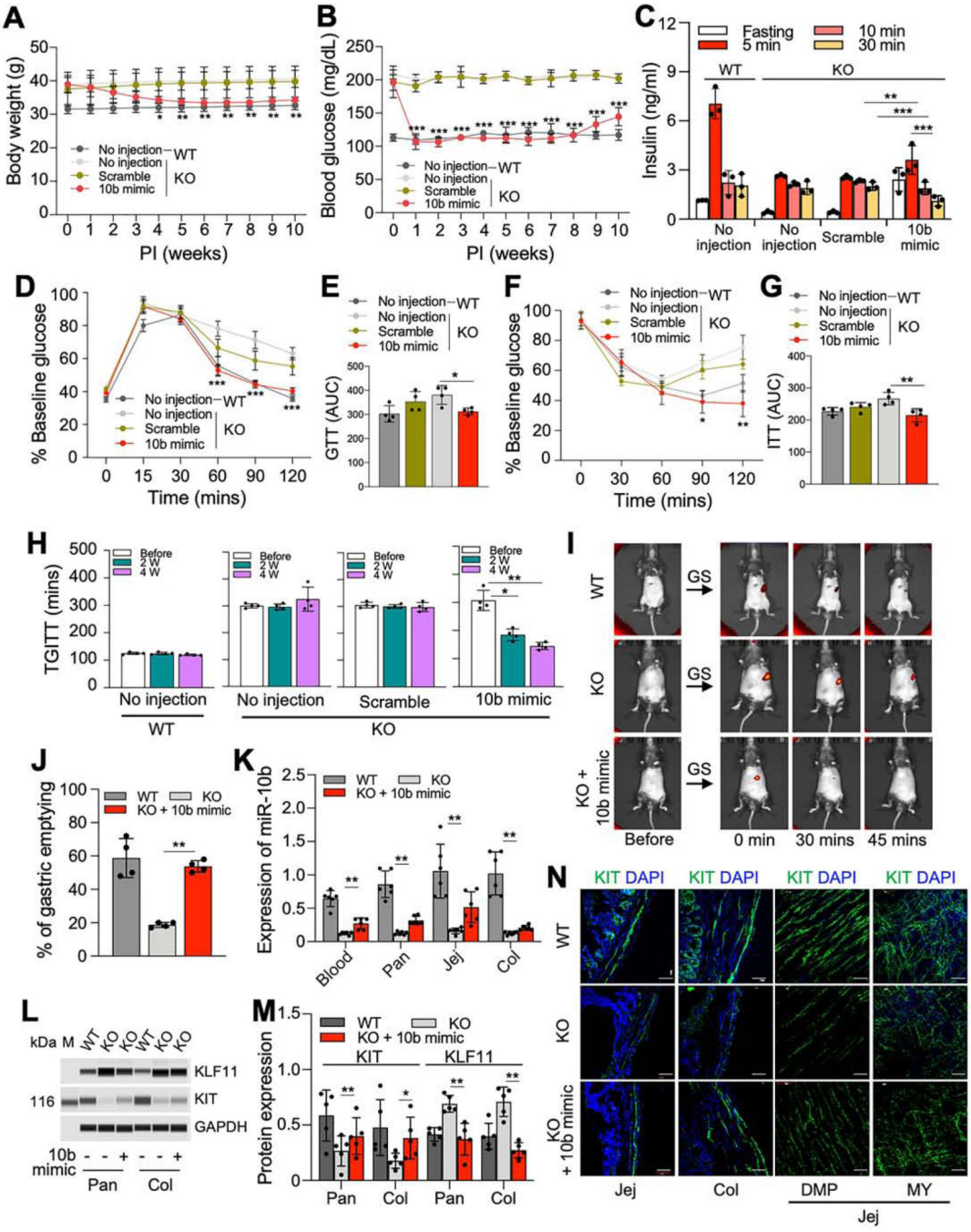

Figure 3.

miR-10b-5p mimic injection rescues the diabetic and GI dysmotility phenotypes in male *mir-10b* KO mice. Male diabetic *mir-10b* KO mice were injected with miR-10b-5p (10b mimic), a negative control (scramble RNA), or given no injection, compared to WT mice. (*A*, *B*) Body weight and fasting blood glucose levels for 10-weeks post-injection (PI). (*C*) Comparison of insulin levels after 6-hrs fasting and after glucose injection in *mir-10b* KO and WT mice at 1-week post-injection (IP) (One-way ANOVA). (*D* and *F*) GTT and ITT at 1-week PI. (*E and G*) GTT and ITT plot of the AUC from (*D and F*) (One-way

ANOVA). (*H, I*) TGITT (One-way ANOVA) at 2- and 4-weeks PI and gastric emptying test at 4-weeks PI. (*J*) Quantification of gastric emptying at 30-min (One-way ANOVA). (*K*) Quantification of miR-10b-5p in the blood, pancreas, jejunum, and colon in male WT and diabetic *mir-10b* KO mice 1-week after 10b mimic or no injection measured by qPCR (One-way ANOVA). (*L, M*) Western blot and quantification of KLF11 and KIT in the pancreas and colon in male WT and diabetic *mir-10b* KO mice 1-week after 10b mimic or no injection (One-way ANOVA). (*N*) Images of cross sections and whole mount tissue sections showing the restoration of ICCs (KIT^+) in the jejunum and colon at 1-week PI. Scale bars are 50 μm. n=3–4 per condition for each experiment. Pan, pancreas; Col, colon; Jej, jejunum; DMP, deep muscular plexus; MY, myenteric plexus. Error bar indicate SEM, Two-way ANOVA (*A-D*). $*p < 0.05$, $**p < 0.01$, $***p < 0.001$.

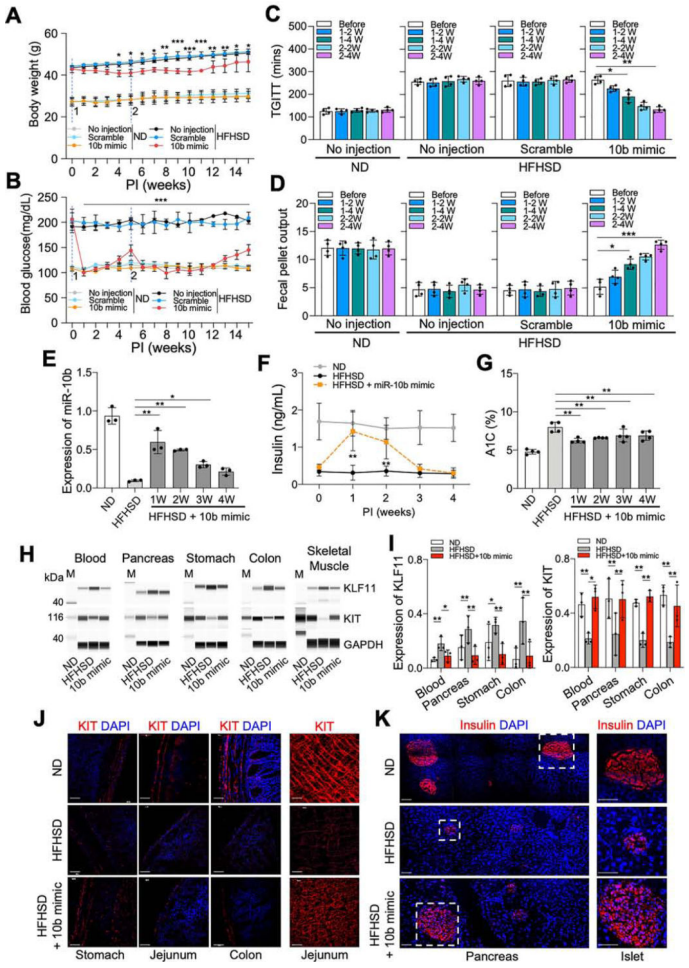

Figure 4.

miR-10b-5p mimic rescues the diabetic and GI dysmotility phenotypes in male HFHSD-fed mice. Male C57 mice (at 4-weeks of age) were fed a HFHSD (diabetic) or ND (healthy controls) for 4-months and injected twice (second injection at 5-weeks) with either the miR-10b-5p mimic (10b mimic), a negative control (scramble RNA), or given no injection, over a 10-week period. (*A*, *B*) Body weight and fasting blood glucose level comparison (Two-way ANOVA). (*C*, *D*) TGITT and fecal pellet output. (*E*) Expression of miR-10b-5p in the blood from ND-fed healthy mice, HFHSD-fed diabetic mice, and 10b mimic-injected HFHSD-fed mice at 1–4 weeks PI measured by qPCR. (*F*) Changes in insulin levels (6-hrs fasting) and A1C levels in male mice fed a HFHSD or ND and injected with 10b mimic (Two-way ANOVA). (*G*) Changes in A1C levels in male mice fed a HFHSD or ND and injected with 10b mimic. (*H, I*) Western blot and quantification of KLF11 and KIT in blood, pancreas, stomach, colon and skeletal muscle from ND, HFHSD, and 10b mimic-injected HFHSD-fed mice at 3-weeks PI. (*J, K*) Images of cross sections and whole mount tissue sections showing the restoration of ICCs (KIT^+) in the stomach, jejunum, and colon, as well as in β cells ($Insulin^+$) in the pancreatic islets at 3-weeks PI. Scale bars are 100 μm. n=3–4 per condition for each experiment. Error bar indicate SEM, One-way ANOVA. $*p < 0.05$, $**p < 0.01$, $***p < 0.001$.

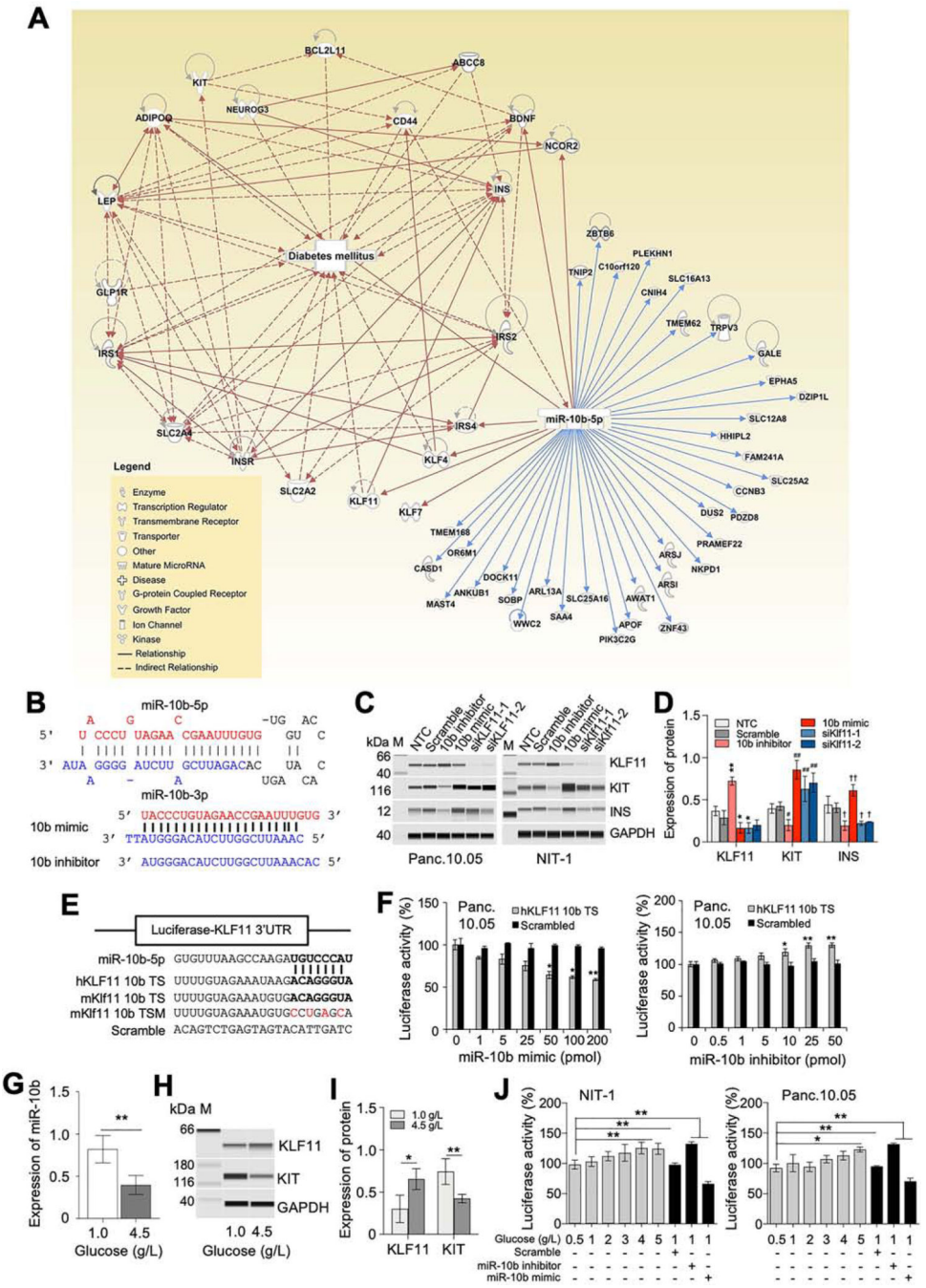

Figure 5.

Target identification and validation of miR-10b-5p *in vitro*. (*A*) Pathway analysis of miR-10b-5p and its target genes associated with diabetes mellitus according to Ingenuity Pathway Analysis. (*B*) The sequence and structure of the mouse miR-10b precursor (pre-miR10b) encoding miR-10b-5p and miR-10b-3p, a synthetic miR-10b-5p molecule (miR-10b-5p mimic) and a synthetic miR-10b-5p antisense molecule (miR-10b-5p inhibitor). (*C*) Targeting of KLF11, KIT and INS by the miR-10b-5p mimic, miR-10b-5p inhibitor, and KLF11 siRNAs (siKLF11–1 and siKLF11–2 in human Panc.10.05 cells and

siKlf11–1 and siKlf11–2 in mouse NIT-1 cells). A non-targeting (scramble) RNA and non-transfection control (NTC) were used as negative controls. A protein marker (M) with corresponding molecular weights (kDa) is shown. (*D*) Quantification of protein expression levels of KLF11, KIT and INS in Panc.10.05 cells. (*E*) Diagram of luciferase reporter plasmids with the miR-10b-5p target site (miR-10b-5p mimic binding site) of human and mouse KLF11 (hKLF11 10b TS and mKlf11 10b TS) and a mutant (mKlf11 10b TSM). (*F*) Target validation of KLF11 with the miR-10b-5p mimic and miR-10b-5p inhibitor in Panc.10.05 cells transfected with luciferase reporter plasmids (Two-way ANOVA). (*G*) Quantification of miR-10b-5p in NIT-1 cells incubated in media with different glucose concentrations (0, 1.0, and 4.5 mg/L). (*H* and *I*) Western blot and quantification of KLF11 and KIT expression at different glucose concentrations. (*J*) Target effects of KLF11 in NIT-1 and Panc.10.05 cells cultured at different glucose concentrations. n=3 per condition for each experiment. Error bar indicate SEM, One-way ANOVA. $*p < 0.05$, $**p < 0.01$.

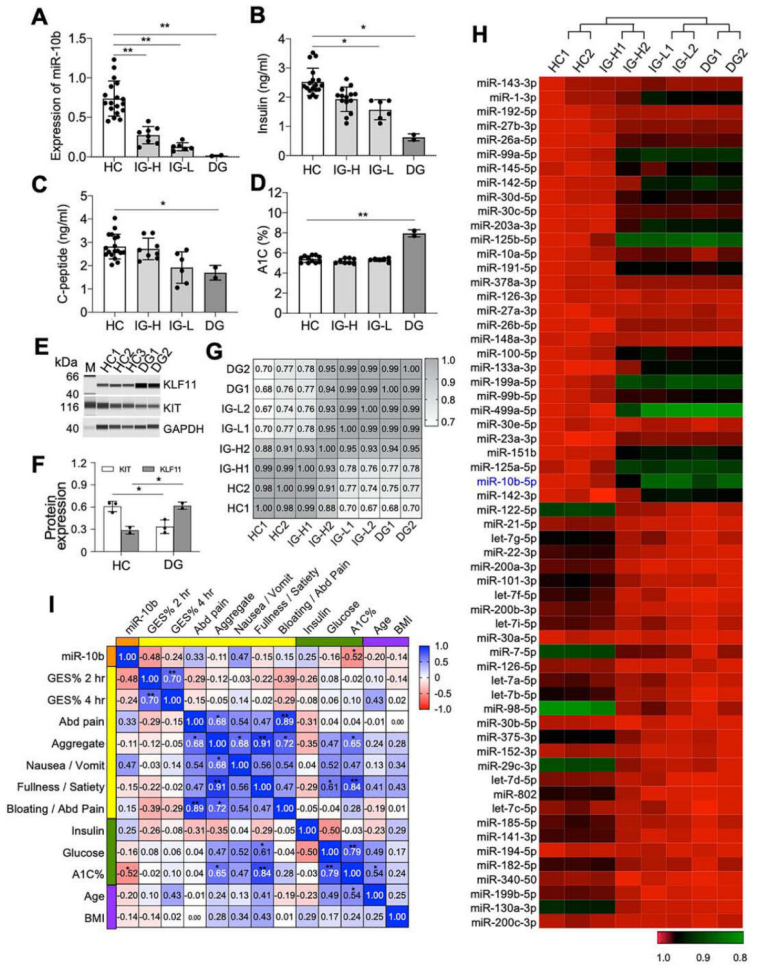

Figure 6.

Validation of altered expression of miR-10b-5p, KLF11, and KIT in patients with idiopathic and diabetic gastroparesis. (*A*) Expression of miR-10b-5p in blood samples collected from idiopathic gastroparesis patients (IG, n=14) and diabetic gastroparesis patients (DG, n=2) compared to healthy control subjects (HC, n=18). The IG group was divided into two groups with high miR-10b levels (IG-H, n=8) or low miR-10b levels (IG-L, n=6). (*B-D*) Comparison of insulin, C-peptide and A1C levels in the blood of the four groups. (*E*) Western blot of KLF11 and KIT in the blood samples of the HC and DG groups. (*F*) Pearson correlation analysis between miRNA-seq data obtained from the blood of HC, IG-H, IG-L, and DG (n=2). (*G*) Heat map of 70 most dynamically regulated miRNAs in blood plasma samples from HC, IG-H, IG-L, and DG (n=2). (*H*) The Spearman rank correlation between miR-10b-5p expression levels and metabolic parameters, clinical GI symptoms, and gastric emptying scintigraphy (GES) % at 2- and 4-hrs in gastroparesis. Error bar indicate SEM, One-Way ANOVA. *$p < 0.05$, **$p < 0.01$.

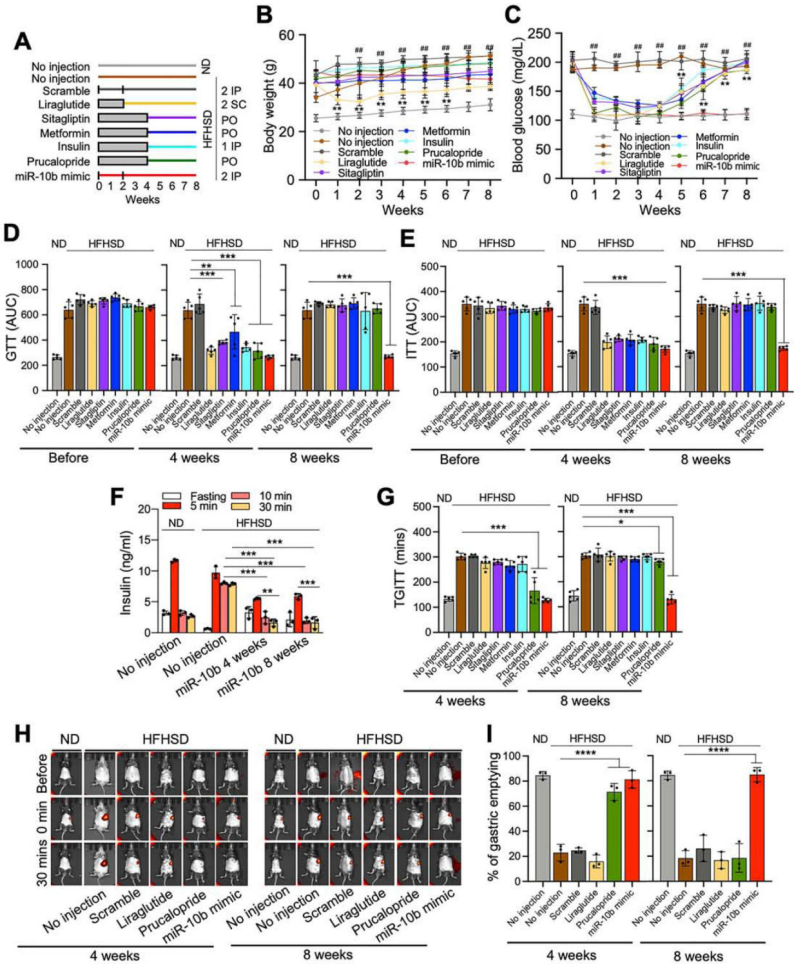

Figure 7.

Efficacy comparison of miR-10b-5p mimic with antidiabetic and prokinetic medicines in HFHSD-fed diabetic C57 male mice. (*A*) A study design of drug effects in HFHSD-fed diabetic mice- or ND-fed healthy mice. miR-10b-5p, or scramble RNA were injected twice, at 0- and 2weeks by IP injection; Metformin or Sitagliptin was provided daily PO for 4-weeks; Liraglutide was injected twice daily by SC injection for 2-weeks; Insulin was injected once daily by IP injection for 4-weeks; Prucalopride was provided daily PO for 4-weeks. (*B, C*) Body weight and fasting blood glucose levels for 8-weeks post treatment (Two-way ANOVA, n=5). (*D, E*) Comparison of GTT and ITT plot of AUC (n=5). (*F*) Comparison of insulin levels at 6-hrs fasting and after glucose injection (n=3). (*G*) TGITT comparison (n=5). (*H, I*) Gastric emptying images and quantification of stomach emptying (n=3). Error bar indicate SEM, One-way ANOVA. *$p < 0.05$, **$p < 0.01$, ***$p < 0.001$, ****$p < 0.0001$, $^{\#}p < 0.05$, $^{\#\#}p < 0.01$.